A R C H I V E S O F M E T A L L U R G Y A N D M A T E R I A L S
Volume 49 2004 Issue 2

D.L. BEKE *, Z. ERDÉLYI*, I.A. SZABÓ*, G.A. LANGER*, G. KATONA*, C. CSERHÁTI*

DIFFUSION IN NANOSCALE

DYFUZJA W NANOSKALI

Mass transport on nanoscale has specific features because of the presence of high number of grain- and interphase boundaries, as well as because of the fundamental problems related to the very short diffusion distances. In the first part examples on the changes (as the micro-metre scale is reduced to nanometre dimensions) of the overall mass transport due to the boundary effects are exposed. Then examples of processes, in which the diffusion coefficient depends strongly on the concentration (non-linearity) and the diffusion distance is typically few nanometres, will be discussed.

Opis transportu masy rozpatrywanego w skali nano posiada swoja specyfikę ze względu na znaczną ilość granic tak międzyziarnowych jak i międzyfazowych oraz na istotne problemy związane z bardzo niewielką drogą dyfuzji. W pierwszej części opracowania przedstawiono przykłady zmian transportu masy związanych z efektami granicznymi (przy przejściu od skali mikro do nano). Następnie dyskutowane są przykłady procesów, w których współczynnik dyfuzji silnie zależy od stężenia i gdy typowa droga dyfuzji wynosi kilka nanometrów.

1. Introduction

Grain boundaries (GB) are, generally, diffusion short circuits. Consequently, the major part of material transport will occur by GB diffusion in nanomaterials where a large amount of atoms can lie on grain or interphase boundaries (50% as well as 20% for grain size equal to 5 nm and 10 nm, respectively). As we will see one of the interesting questions is related to the classical classification [1,2] into the well-known type *A*, *B* and *C* regimes of *GB* diffusion. This classification fails in nanomaterials, even if it contains only one type of short circuits with one diffusion coefficient only [3], because the B regime can not be realized and

* DEPARTAMENT OF SOLID STATE PHYSICS, UNIVERSITY OF DEBRECEN, 4010 DEBRECEN, P.O.Box.2, HUNGARY

a variety of the possible sub-regimes can be treated ((C-C, B-B, AB-B, A-B sub-regimes as compared to the classical division for *A*, *B* and *C* regimes) and investigated experimentally [4,5]. Similarly segregation effects can also be different form the well-known microcrystalline case [3,6].

Diffusion in nanostructures presents challenging features even if the role of structural defects (dislocations, phase- or grain-boundaries) can be neglected. This can be the case for diffusion in amorphous materials or in epitaxial, highly ideal thin films or multilayers where diffusion along short circuits can be ignored and "only" fundamental difficulties, related to nanoscale effects, raise. For example the continuum approach can not be automatically applied [3,6].

In this paper, based on the research experience of our group, most of the above challenging phenomena will be exposed and/or discussed in more details.

2. Role of structural defects (grain- and interphase-boundary effects)

If the *role of structural defects* (dislocations, phase- or grain-boundaries) is important, a set of interesting phenomena can be observed even if the nanomaterial contains only one type of short circuits with one diffusion coefficient only [3]. It is well known from the classical treatments (e.g. [1,2]) that there are three different GB diffusion regimes: type *A*, *B* and *C*. *For grain sizes, d, in the order of 10 nm the A or C regimes will be more important and the B regime* – in contrast to micro-crystalline samples where it is the most frequently realized case – *can not be observed.* It can be seen from the condition for type B regime [1,2] ($100\delta < L = (Dt)^{1/2} < d/20$, where δ ($\cong$0.5nm) is the *GB* thickness and t is the time of diffusion), that if $d \cong 10$ nm this condition can not be fulfilled. Thus, according to the conditions for the type *A* and *B* regimes ($L \gg d$ for *A* and $20\,L < \delta$ for *C*) – depending on t -, either *A* or *C* regimes will be observed. In type *A* regime – according to classical handbooks on diffusion [7] – a significant enhancement of intermixing or solid state reactions is observed, with an effective interdiffusion coefficient given by the Hart's equation [1,7]:

$$D_{eff} = gDg + (1-g)D \tag{1}$$

where g is the grain-boundary volume fraction ($g \approx \delta/d$; the factor of proportionality depends on the grain shape, but is in the order of unity). If $d \cong 10$ nm, then only the first term will be dominant, since usually $Dg/D > 10^4$. Very recently Belova and Murch [8] have shown that that for the estimation of this effective diffusivity the generally accepted Hart equation should be replaced by the Maxwell equation (known from the random resistor network problem) on nanoscale (in order to avoid an overestimation by about 50%):

$$D_{eff} = D_g[(3-2g)D + 2gD_g]/\{gD + (3-g)D_g)\}. \tag{2}$$

It was also found from Monte Carlo simulations that the usual condition for type *A* regime is too stringent and the transition occurs already at $L \cong 0.2d$.

Accordingly, in *A* regime a high effective diffusion coefficient will characterize the rate in any technically important interdiffusion or solid state reaction process (e.g. in surface alloying). On the other hand in many cases the process will take part dominantly along grain- or phase boundaries (type *C* regime) leading to phenomena such as degradation of multilayers by grain-boundary grooving, pinhole formation and coarsening [9,10], or solid state phase transformations in thin films.

Additionally, if there is a multi- level organization in the structure (at least two different types of boundaries are present: e.g. closed free surfaces and GBs in vacuum condensed nanomaterials), then the above clear classification falls even in microcrystalline materials (see. e.g.[1,4,5]). For example the measurements in type *B* regimes can not be simply interpreted by one straight line on the *lgI* (I is the specific activity) versus $y^{6/5}$ plots, but – because of the presence of different type of GBs with different diffusion coefficients – a non-linear penetration plot is usually observed [11,12]. The most recent and more precise treatment of the problem can be found in [4,5] where *intermediate regimes between the A, B and C type diffusion regimes* were defined due to the presence of grain- and interagglomerate boundaries in nanocrystalline γ-FeNi [4,13].

It is also an interesting question: Whether *the GB diffusion coefficients* measured in these alloys *are identical to those obtained in microcrystalline state* (e.g. from diffusion experiments made in type *B* regime) *or not*? There is an increasing number of experimental evidences that the above diffusion coefficients agree very well with each other, i.e. in most of the cases the structure of GBs in nanocrystalline and polycrystalline samples is very similar, provided that the grain-boundary structure is already relaxed [3].

In hetero-diffusion experiments *segregation effects* describing the matching conditions between the diffusion source and the GB (as well as between the GB and the free surface, if there is a terminal free surface present in the experiment) should also be taken into account [5,8,14,15,16]. Usually the segregation kinetics is also a process during which the redistribution takes place along distances of few nanometers. Besides of these kinetic effects, there is also a size effect manifested in changes of the character of the segregation isotherm itself. This is the consequence of the finite size of the sample: either the surface perturbed regions can overlap and thus an increase in the solubility limit can be observed [6], and/or the number of sites at interface can be higher than the number of solutes in the sample and a change form the Fowler-Guggenheim- to a McLean-type [6] (or even to the Henry-type) isotherm [17,18] can be observed.

At short diffusion distances in interdiffusion, leading to formation of reaction products, the usual *parabolic law of diffusion can be violated,* if the role of reactions at the interface is taken into account. At short diffusion times the growth of the reaction layer will be controlled not by a parabolic, but by a linear law according to the formula [7]:

$$x^2 + Ax = Bt, \tag{3}$$

where x is the thickness of the reaction layer, A and B are proportional to the reaction rate and interdiffusion coefficients, respectively. The same effect can be observed in many bulk or surface coarsening processes (Ostwald ripening of ensembles of nano-clusters or beaded

films on a surface, if their characteristic distance is large enough to produce a diffusion interacting ensemble but shorter than the characteristic length, defined above).

It is also well-know, that *the nucleation of a new phase* always needs a certain critical size, d_c, which is typically in the nanometer range. If, for example, in a solid state diffusion reaction the width of the diffusion zone, L, is less than d_c the given phase cannot form [19]. In case of more than one diffusion product this can lead to different interesting observations in the first stages of the heat-treatments.

Sometimes – e.g. in diffusion in MBE (Molecular Beam Epitaxy) grown thin films or multilayers – the diffusion distances can be shorter than the typical distance between the sources and sinks of diffusion vehicles. While in "normal" diffusion *the equilibrium concentration* of such *defects* are set by the sources or sinks (and the characteristic distance, l, between them is much shorter than the macroscopic diffusion length, L), if $L<l$ the mechanism of diffusion can change, similarly as it was already observed, on more macroscopic scale, for diffusion in dislocation free Si single crystals [20].

Bokstein and his co-workers [5,21,22] illustrated that *the mechanical stress field* (both the stress gradient and its hydrostatic component) *can have a considerable influence on the GB diffusion in thin films.* The effect of the stress gradient and the effect of the hydrostatic component can be separated as "gradient effect' and "mobility effect". In [21] the authors argue that the mechanical stress can reach as high values as 1 GPa and the small film thickness can lead to large gradients as well. Furthermore at low temperatures the stress relaxation can be hindered and the hydrostatic component of the stress field can also enhance or supress the grain boundary diffusion (across the exponential dependence of the mobility on the pressure). At the moment there is lack of equivocal evidences for explanations of the existing order of magnitude differences of the grain boundary diffusion coefficients measured e.g. in thin films on different substrates (and thus being in different stress states), although the above explanation offers a plausible solution.

3. Fundamental difficulties

For diffusion in amorphous materials or in ideal bi- or multilayers, where diffusion along short circuits can be ignored, "only" fundamental difficulties, related to nanoscale effects, raise. The most important difference, compared to diffusion along long distances (orders of magnitude longer than the atomic spacing, a), is that the continuum approach can not be automatically applied and there is a gradient energy correction to the driving force for diffusion. This correction becomes important again if large changes in the concentration take place along distances comparable with a, and results in an additional term in the atomic flux, proportional to the third derivative of the concentration. It was shown recently in our group [3,6,9,23-30], that these effects can lead to unusual phenomena especially if there is a strong non-linearity in the problem i.e. if the diffusion coefficient has a strong concentration dependence.

3.1. Basic equations

For exchange mechanism in a binary AB alloy (consisting of a slab of material with N lattice planes, normal to the y axis and each atom in a plane has z_1 nearest neighbours in this plane as well as z^v in planes adjacent to this), with the coordination number $Z = z_1 + 2z_v$ the change in relative concentration of B in plane i is given by (see e.g. [6])

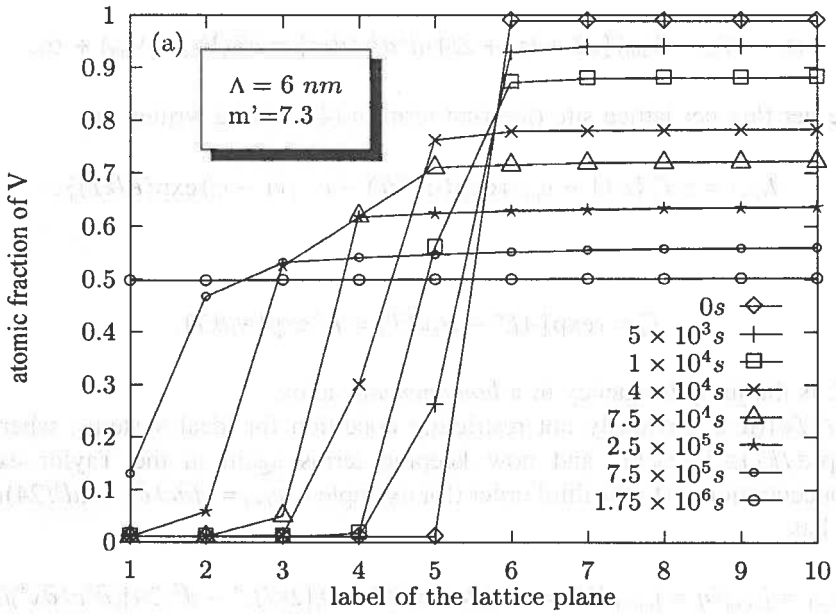

Fig. 1. Concentaration distributions at different times in Mo-V system (m' = 7.3) [23] at T = 1053 K and for Λ = 6 nm

$$dc_i/dt = -z_v[c_i(1-c_{i-1})\Gamma_{i,I-1} - (1-c_i)c_{i-1}\Gamma_{i-1,I} + c_i(1-c_{i+1})\Gamma_{i,i+1} - c_{i+1}(1-c_i)\Gamma_{i+1,i}]. \quad (4)$$

where e.g. $\Gamma_{i,i+1}$ gives the exchange frequency of a B atom in layer i with an A atom in layer $i+1$. Assuming an Arrhenius–type temperature dependence of the jump frequencies ($\Gamma_{i,i+}{}^{1} = \nu\exp[-E_{i,i+1}/kT$, with the attempt frequency ν), an appropriate choice of the activation energies $E_{i,i+1}$ can be such [3,6,24,31] that

$$E_{i,i+1} = E^v - \alpha_i + \varepsilon_i \quad \text{and} \quad E_{i+1,i} = E^v - \alpha_i - \varepsilon_i, \quad (5)$$

where E^v is the saddle point energy and α_i and ε_i are functions of $c_{i,-1}$, c_i, c_{i+1} and c_{i+2} [3,6]:

$$\alpha_i = [z_v(c_{i-1} + c_{i+1} + c_i + c_{i+2}) + z_l(c_i + c_{i+1})](V_{AA} - V_{BB})/2 \quad (6)$$

and

$$\varepsilon_i = [z_v(c_{i-1} + c_{i+1} - c_i - c_{i+2}) + z_l(c_i - c_{i+1})]V. \quad (7)$$

Here V_{AA}, V_{BB} and V_{AB} are the pair interaction energies and the interaction energy, V, has its usual meaning ($V = V_{AB} - \{V_{AA} + V_{BB}\}/2$).

Furthermore, if the surface concentration, $n = cd/\Omega$ (Ω is the atomic volume and d is the distance between the atomic planes), is expanded in Taylor series (up to the third order) and the relations $(c_{i-1})-(c_{i+1}-c_{i+2}) = (d^2)\partial^2 c/\partial x^2$ and $c_i + c_{i+1} = (d/2)\ \partial^2 c/\partial x^2 + 2c$ are also used [6,30];

$$\alpha_i = (V_{AA} - V_{BB})\{cZ + (z_v + Z/4)d^2\partial^2 c/\partial x^2\} = cZ(V_{AA} - V_{BB}) + \alpha_i. \qquad (8)$$

Thus the net flux per lattice site (the first term in (4)) can be written as

$$J_{i,i+1} = z_v \Gamma_i \{c_i(1 - c_{i+1})\exp(-\varepsilon_i/kT) - c_{i+1}(1 - c_i)\exp(\varepsilon_i/kT)\}. \qquad (9)$$

with

$$\Gamma_i = \nu\exp[-(E^v - \alpha_i)/kT] = \Gamma_i^h \exp[\alpha_i/kT]. \qquad (10)$$

Here Γ_i^h, is the jump frequency in a *homogeneous* alloy.

If $\varepsilon_i/kT \ll 1$(it is obviously not restricting condition for ideal systems, where $\varepsilon_i = 0$) then $\exp(\varepsilon_i/kT) \cong 1 + \varepsilon_i/kT$, and now keeping terms again in the Taylor expansion of the concentration up to the third order (for example $c_i - c_{i+1} = -d\partial c/\partial x - (d^3/24)\partial^3 c/\partial x^3$) [6], one has

$$j_{i,i+1} = j_{i,i+1}/q = j_{i,i+1}d/\Omega = -D_i(\partial c/\partial x)/\Omega + D_i[2\kappa/f_o'' - d^2/24](\partial^3 c/\partial x^3)/\Omega \qquad (11)$$

where q is the area of the specimen perpendicular to the direction of diffusion. In (11) D_i is the intrinsic diffusion coefficient, $D_i = z_v d^2 \Gamma_i \theta$, θ is the so called thermodynamic factor [32] and $\theta = 1 - 2ZVc(1-c)/kT$ i.e. for an ideal system $\theta = 1$. κ and f_o'' are the gradient energy coefficient and the second derivative of the free energy of the homogeneous system [7,32], respectively.

Expression (11) – except for the second term proportional to d^2 in the bracket – is similar to the well-known Cahn-Hilliard expression [6,32]. However, while the classical Cahn-Hilliard expression contains a diffusion coefficient belonging to a *homogeneous* alloy, here in the exponent of D_i the α_i' is proportional to the second derivative of the concentration (see eq. (8)), i.e. inhomogeneity corrections lead not only to the term proportional to the third derivative of concentrations, but also to an additional factor in D_i!

For ideal solutions, where $V = 0$ and thus $\kappa = 0$, the presence of the term proportional to d^2 (because of its negative sign), would lead to composition oscillations (D is positive – and if it is independent of composition – the sign of the second term corresponds to $2\kappa/f_o'' < 0$ "Cahn-Hilliard" term but with $f_o'' > 0$ [32]). This is possibly due to the simplifications made during the transition from the discrete model to the continuous one (see also [6]). Nevertheless, the role of these refinements would need more attention if diffusion takes place on nanoscale and one uses continuum equations. One can expect for example that

from the solutions of equation (11), solutions with wavelength $\Lambda \leq 2d$ should be excluded (the oscillations take place with a concentration wave of $\Lambda = 2d$). For composition dependent D the situation can be even much more complex. These remarks can be important in the description of nanodiffusion in amorphous systems (see also [3]), where no discrete models are available and one can rely only on the "improved" continuum equations.

For concentration independent jump frequencies $\Gamma_{i,i+1} = \Gamma_{i+1,i} = \Gamma$ and the Fick II. law (eq. (4)) has the form:

$$\partial c_i / \partial t = \Gamma (c_{i+1} + c_{i-1} - 2c_i). \tag{12}$$

The term in the bracket, divided by d^2, can be easily rewritten to the second derivative of the relative concentration. Now, it is easy to show [7] that taking a sinusoidal concentration profile ($c \sim \sin\{2\pi x/\Lambda\}$) the solutions of the continuum Fick equation and (12) will be identical only for $\Lambda > 10$d. However, in the case of a strongly composition dependent interdiffusion coefficient the validity limit of the continuum approach – even in an ideal system – can be shifted to larger length by about one order of magnitude [24], i.e. it will be in the order of 10 nm. These results were obtained in [24] by carrying out calculations for diffusion intermixing in multilayers of ideal solid solutions, from the discrete model as well as from the continuum Fick II. equation by finite volume calculations with diffusion coefficients equivalent to that used in the atomic model. The strength of the composition dependence of D in the continuum model is measured by m' defined as

$$\log D(c) = \log D(0) + \text{m'c}. \tag{13}$$

In the discrete model (see also the first term in eqs. (8) as well as eq. (10)) $m = Z(V_{AA} - V_{BB})/kT$ and in the calculations of [24] m' (m' = m lg$e$) was 7.3 (Mo/V system).

3.2. Results of simulations and experiments

3.2.1. Homogenization by the shift of the interface

It was obtained in [23], from finite volume calculation of the solutions of (4) in Mo/V multilayers, that for a strong concentration dependence of $D_{Mo} = D_V = D$ the interface between the *Mo* and *V* remains atomic sharp and shifts as a whole until the component with small D has not been consumed (Fig.1). It can also be seen that the diffusion is very asymmetrical: there is a fast dissolution and diffusion of Mo into *V*, but there is no diffusion in *Mo*. This behaviour, as it is illustrated in Fig. 2, was indeed observed very recently in amorphous Si/Ge system by Auger-depth profiling technique [25] (in both systems is $V \cong 0$.)

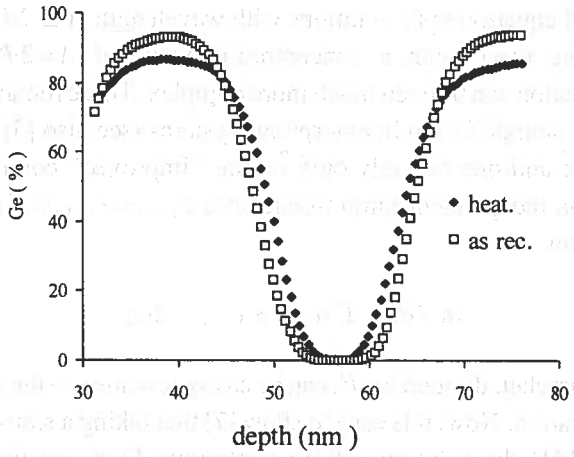

Fig. 2. Auger depth profiles for the as-received and annealed (at 680 K for 100 h) amorphous Si/Ge multiplaxer [25]. The Si content increases in Ge and the Si layer shrinks

3.2.2. Non-parabolic shift of sharp interface in ideal systems

The non-linearity (strong composition dependence of D) can lead to even more interesting results if we have dissolution of a thin film into a substrate [26]. Fig. 3. shows the results of simulations carried out for Ni dissolution into Cu (again the system is ideal, i.e. $V=0$). It can be seen that the dissolution starts at the interfacial layer, and until this is not consumed, the next layer remains complete. Thus the interface shifts step by step. This layer-by-layer dissolution takes place until the moving "interface" reaches the Ni layer just before the last. Then, due to the driving force for surface segregation, the intermixing will be continued by the saturation of Cu in the top layer and the change in the second layer will be retarded according to the segregation isotherm. The layer-by-layer dissolution – if the substrate is semi-infinite and the diffusion coefficient depends strongly on the concentration [26] – results in a periodic behaviour as a function of time: each plane practically dissolves subsequently reproducing the same process. Therefore *the average value of v should be constant, independent of time, and the interface shifts linearly with time, which is in contrast to the parabolic law ($v \propto t^{-1/2}$) would be expected from a continuum model.* Of course, after the dissolution of more and more layers one will have a transition to the parabolic dissolution. Obviously, this transition will depend on the value of m' [26]. Fig. 4a. shows the position of the interface versus time, obtained from simulation for a semi-infinite Cu(111) substrate with 100 atomic layers of Ni. Due to the periodicity, mentioned above, the curve has periodic oscillations around the straight line fitted, but the slope of the straight line is $1 \pm 8\times10^{-4}$, i.e. the average shift is indeed linear. It was also shown by simulations that already for 1000 atomic layers and at longer times the dissolution is indeed obeys the parabolic law [6,26].

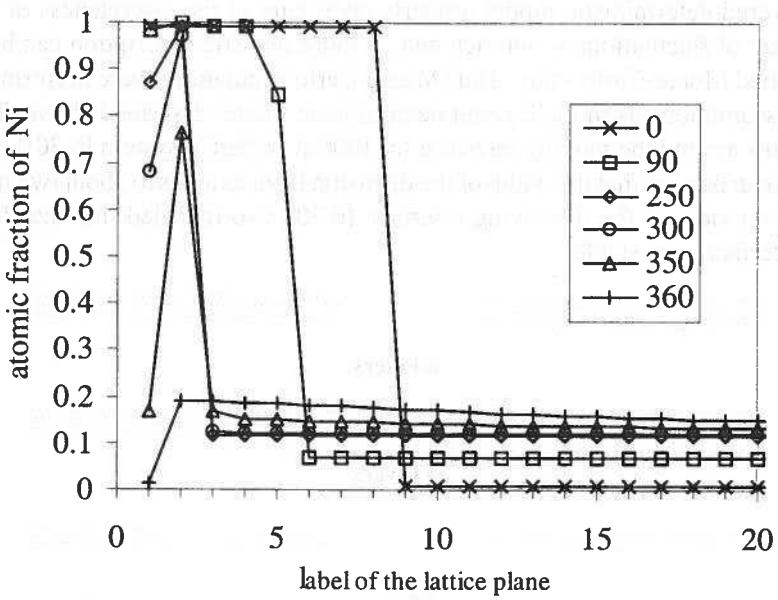

Fig. 3. Concentration profilesfor Ni dissolution into 51 layers of Cu(111) (of which only 12 is shown here) for different times (given in special untis [26])

Although the oscillating character of the dissolution – because of technical difficulties – could not be resolved experimentally in [26], the above simulation result was confirmed by measuring the kinetics of the Auger signals of Ni and Cu from the top of the 8 monolayer Ni. Fig. 4b. shows the final results for the average time evolution of the Ni thickness versus time for 679 K. It can be seen that n is indeed a linear function of time up to the second layer.

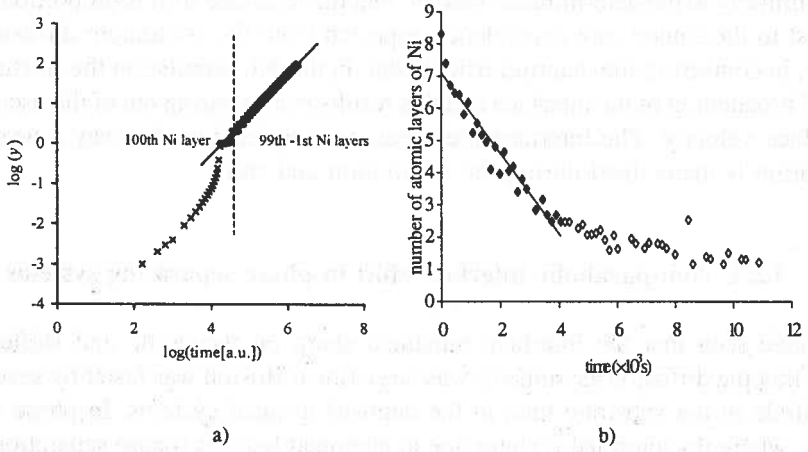

Fig. 4. a): Position of the interface versus time for the dissolution of 100 Ni layer into Cu(111) substrate (see also the text), b): Change of the Ni thickness at 679 K [26]

The layered deterministic model properly takes care of the discreteness of the lattice, but the effect of fluctuations is not included. A more realistic description can be achieved with a detailed Monte-Carlo study. Thus Monte-Carlo simulations were performed [6] with the same assumptions as in the layered deterministic model described above. The atomic arrangements around the moving interface (at 1000 K in Ni/Cu system [6,30]) can be seen on Fig.5. It can be seen that the width of the diffusion front extends to about two monolayers only. The top view of the dissolving interface [6,30] also revealed that the shape of the moving interface was stable.

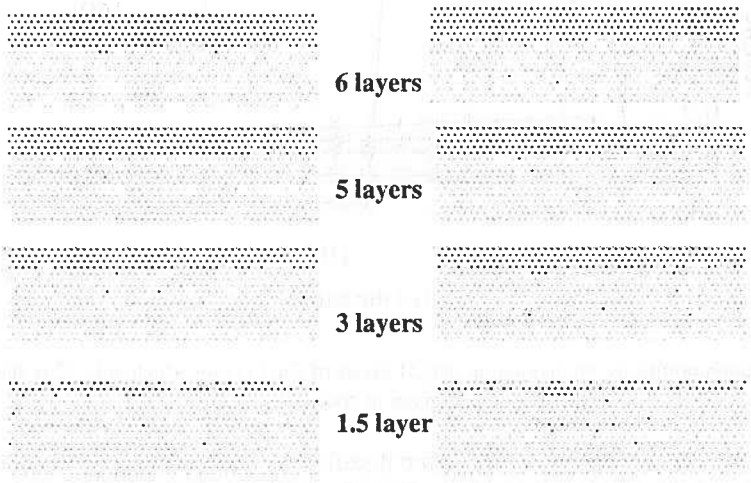

Fig. 5. Cross-section of the sample at different times in two MC simulation runs [6]. The black and gray dots represent different atoms

In conclusion, after taking into account the fluctuations by MC simulation, we have found – similarly to the deterministic model - that the interface shift is proportional to time, in contrast to the square root dependence expected from the continuum diffusion model. However, in contrast to the deterministic model, in the MC simulation the fluctuations led to a small broadening of the interface and this results in a smearing out of the oscillations of the interface velocity. The interface preserves its shape and in this way a nearly steady configuration is maintained during the dissolution and shift.

3.2.3. Non-parabolic interface shift in phase separating systems

We have seen that the interface remained sharp on nanoscale and shifted linearly provided that the diffusion asymmetry was large (the diffusion was faster by several orders of magnitude in the substrate than in the deposit) in ideal systems. In phase separating systems – where the interface is sharp due to chemical reasons (phase separation) – it was obtained from previous computer simulations [33-35] that the interface displacement was proportional to the square root of the time. However, in these simulations the composition

dependence of the diffusivity (diffusion asymmetry) was neglected. Thus it was very plausible to study the interplay of the diffusion asymmetry (composition dependence of diffusion coefficient) and the phase separation tendency (chemical effect) in the kinetics of the interface shift during dissolution in a binary system with restricted solubility. In [29] we have demonstrated by computer simulations (in fcc structure for 111 plane; $z_l = 6$ and $z_v = 3$) how these parameters could influence the kinetics of the interface motion.

The position of the interface was fixed to the plane with the composition 0.5 (it can obviously lie between two atomic planes). After determining this position, logarithm of the shift versus the logarithm of the time was plotted. Fitting a straight line to the data (which implies power law behaviour: $y \propto t^{k_c}$), its slope gave the power of the function describing the shift of the interface (it is called *kinetic exponent* and denoted by k_c). Obviously for parabolic interface shift $k_c = 0.5$. Since we wanted to demonstrate the effects of the composition dependence of diffusion coefficients as well as the phase separation tendency on the kinetics of the interface shift, the parameters m' and V (or V/kT) were changed during the calculations.

Figure 6a shows the initial values of the kinetic exponent, k_c, (obtained by fitting to the interval corresponding to the dissolution of the first five atomic planes) versus V/kT for different m' values. It can be seen that k_c is almost constant and, as it is expected, it is very close to 0.5 for small m' (week composition dependence of the diffusion coefficients). At the same time, the deviation from the square root kinetics increases with increasing m' for a fixed value of V/kT. The deviation from the parabolic law is again a real "nano-effect", because after dissolving a certain number of layers (long time or macroscopic limit), the interface shift returns to the parabolic behaviour independently of the input parameters (see Fig. 6b).

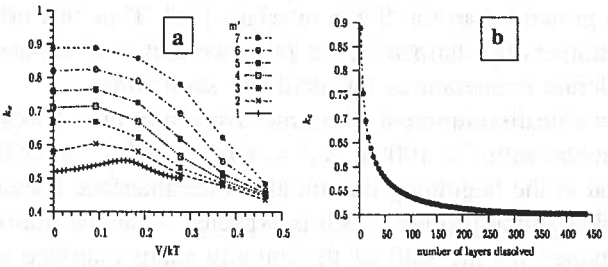

Fig. 6. Initial value of the kinetic exponent versus V/kT for different m' values [29], b): Change of k_c during dissolution ($m' = 7$, $V/kT = 0.09$). The more layers are dissolved the closer the value of k_c to 0.5 is

On the basis of our previous results on the linear shift of a sharp interface in ideal binary systems, obtained by Monte Carlo simulations, it is expected that the above conclusions (drawn from the deterministic model) on the non-linear interface shift in phase separating systems remain valid including the fluctuations as well.

Thus Fig. 6 reflects an interplay of two effects: i) the change of k_c due to the gradient energy effects scaled by V/kT, ii) the change of k_c due to the diffusion asymmetry measured

by m'. This latter nano-effect – similarly to the case of the shift of the interface in an ideal binary system – as it can be seen in Fig.6b, should diminish for long diffusion distances/times.

3.2.4. Sharpening of an initially diffuse interface in ideal binary systems

Another interesting feature obtained again by the same type of model calculations and also by Monte Carlo technique [27], is that an initially wide A/B interface can become sharp on nanoscale even in an ideal system. While such a process is obvious in an alloy with large miscibility gap (the metastable solid solution in the smeared interface region decomposes and a sharp interface is formed), it is surprising at first sight in systems with complete mutual solubility, because according to the macroscopic Fick I law the direction of the atomic flux is always opposite to the direction of the concentration gradient. Indeed, for composition independent D, the concentration profile will gradually decay and only a flattening of the (sharp or broadened) interface, produced experimentally, is generally expected.

The problem is interesting not only from fundamental point of view, but has technological importance as well. The Ni/Cu system for example is a model material for giant magnetoresistance (GMR), and in these systems the abruptness of the interface, and the knowledge of the possibilities for their improvement, is a key point. Furthermore, multilayers made of Mo and V (which is also an ideal binary system) are model materials for X-ray mirrors, or Si/Ge systems are basic semiconductor structures, where again the sharpness of the interfaces can be very important requirement for many applications. It is also well known that in Si-Ge multilayers grown by MBE the Ge/Si interface, produced by the deposition of Si on Ge, is always less sharp (due to the mixing driven by the segregation of Ge during the growth) than the Si/Ge interface [36]. Thus this effect offers a way to improve the multilayers by sharpening the interface and to eliminate the asymmetry by annealing at moderate temperatures for relatively short times.

Figure 7a shows the dissolution of 10 atomic layers of A into a bulk B(111) semi-infinite substrate (fcc structure with T = 1000 K, V_A^A = -074 eV and V_B^B = -058 eV i.e. for m' = 9). It can be seen that at the beginning the initially wide interface becomes more and more sharp. After the sharpening process – as it is expected – the dissolution takes place in the same way as obtained for the shift of the initially sharp interface above: the interface remains atomic sharp and shifts step-by-step. The process clearly reflects the asymmetry of the diffusion: there is practically no diffusion in pure A and the diffusion is a very fast in pure B, leading to a gradual sharpening of the composition profile.

As it was already mentioned an initially abrupt interface can remain sharp during diffusional intermixing in multilayers as well (see Fig. 1). Therefore, it is an interesting question whether an originally wide interface can also become sharper in multilayers. The situation differs from the dissolution of a thin film into semi-infinite substrate: the most important effect is that Ni atoms can saturate the Cu layer, and this leads to the change of the diffusivity there. However, as Fig. 7b shows, the first part of the process is the interface

sharpening in this case as well, after which the interface shifts step-by step and just after consuming of the whole Ni layer complete homogenization takes place.

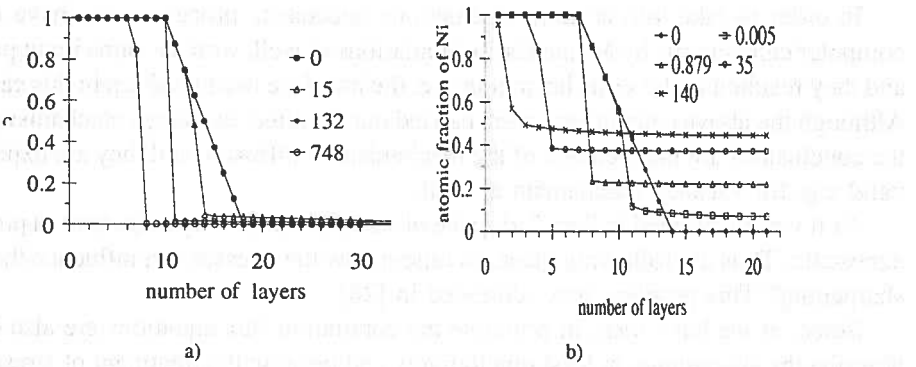

Fig. 7. a): Sharpening of the initially linear concentration profile of Ni during interdiffusion with Cu [27]. b): 16 Interface sharpening in an A/B multilayer system. (Time units shown must be multiplied by 10^6)

The above result gives also a plausible explanation for the apparent contradiction with the continuum Fick I law:

$$\mathbf{j} = -D\,grad\,\rho, \tag{14}$$

where ρ is the density ($\rho = c/\Omega$). Since in ideal binary systems D has a positive value and, for concentration independent diffusion coefficients, this equation should lead to flattening of the interface. If the concentration gradient is constant along the interface it is only D on which the absolute value of the atomic flux depends. Therefore the 'flux distribution' follows the $D = D(c)$ function and thus even the continuum flux equation is capable to describe some sharpening.

Obviously at longer annealing times – as it is expected from general thermodynamics – homogenization should take place. Indeed this is the case for the multilayer sample: although at the beginning the process decreases the gradient by filling up of layer Cu with Ni (and not by flattening of the interface), the final state is the completely intermixed homogeneous alloy. For the case of semi-infinite geometry the first part of the intermixing (the initial sharpening and linear shift of the interface) will be extended to times under which the deposited film consumes. Of course for thick films, before reaching this stage, the kinetics of the dissolution will gradually change from linear to parabolic (as we have seen before), and this transition time will be determined by the "strength" of the concentration dependence of the diffusion coefficient, m'. For m' = 0 the "normal" intermixing with the formation of a symmetrical diffusion profile will take place, while with increasing m' the diffusion profile will be more and more asymmetrical and finally the above discussed effects can be observed on nanoscale.

It is important to note that m' is inversely proportional to the temperature (see the text below eq. (13)), and thus with decreasing temperature it is easy to reach those values for

which the above non-linear effects can be observed. Indeed, as it can be checked from the known pair interaction energies or from the experimental D values, it is very general that at low temperatures m' is large enough that the sharpening of the interface is expected.

In order to take into account fluctuations (stochastic processes) we have performed computer calculations by Monte Carlo simulations as well, with the same input parameters, and they resulted in the same behaviour, i.e. the interface became sharp in this case as well. Although the above calculations were carried out for direct exchange mechanism of atoms, the conclusions are independent of the mechanism of diffusion and they are expected to be valid e.g. for vacancy mechanism as well.

As it was mentioned in Sec. 2, the role of stresses can be very important in processes on nanoscale. Thus the following question raises: how the stresses can influence the interface sharpening? This problem was addressed in [28].

Since, as we have seen, in principle the continuum flux equations are also capable to describe the sharpening, at least qualitatively and because the treatment of stress effects is not well developed for the discrete, atomistic kinetic approach [32], computer simulations were carried out in the framework of Stephenson's continuum model [37] for Mo-V multilayer system. Exponential composition dependent diffusion coefficients were used and it was assumed that $D_v = 2D_{Mo}$. The modulation length of the multilayer was 6 nm, the initial 'wideness' of the interface between the Mo and V layers was 1 nm. Fig. 8 shows the time evolution of the composition profile when all the stress effects are ignored, and beside the 'filling-up' of V by Mo, there is indeed interface sharpening, similarly as observed above in the discrete model. The time scale is normalized; t_r is the stress relaxation time (corresponding to a simple Newtonian flow; $t_r = 6\eta(1\text{-}\nu)/E$; η the viscosity, E the Young modulus and ν the Poisson ratio, respectively).

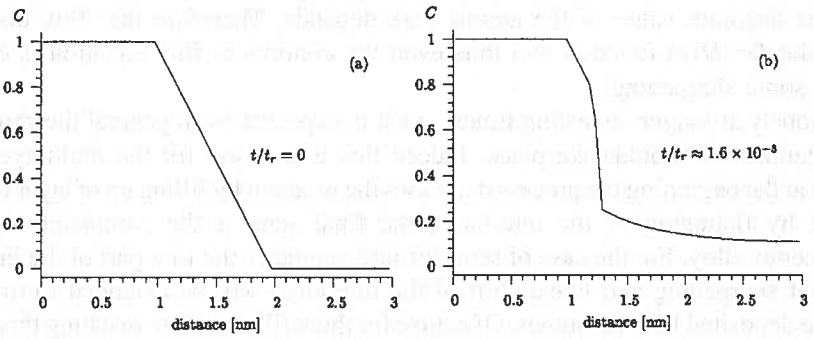

Fig. 8. Time evolution of the composition profile of Mo, at two different normalized times, when all the stress effects are ignored [28]

In Fig. 9 the sample initially is stress free and during mixing a stress peek develops on the Mo side close to the interface and on the V side an almost homogeneous stress field (with opposite sign) appears. This is because the Mo atoms near the interface can easily dissolve into the V and diffuse there, whereas the V atoms practically cannot penetrate into the Mo (diffusion asymmetry due to the strong composition dependence of D_i).

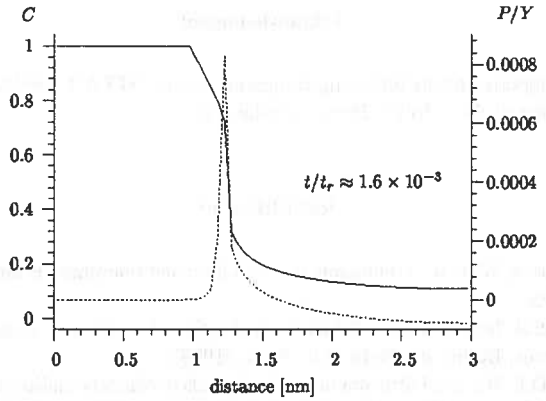

Fig. 9. Time evolution of the composition profile of Mo at $t/t_r = 1.6 \times 10^{-3}$ when only the diffusional stress ($D_V/D_{Mo} = 2$) is taken into account (The initial state is the same as in Fig. 8. The dotted line is the normalized pressure (P/Y)

In order to illustrate stronger stress effects, in Figure 10 the dashed line corresponds to five times larger volume flow (the diffusion induced stress is determined by the net volume flow caused by the differences of D_i). It can be seen that in the second case a slowing down effect is already visible, but the sharpening is still present (obviously with a slower rate). The slowing down effect is due to the presence of the pressure peak in the Mo side just at the sharp interface formed (see e.g. Fig. 9). The pressure peak shifts with the moving interface and there is a steady state during which the height of the pressure peak is almost constant (it decreases only because of the finite size of the V layer). The presence of the stress gradient, due to this peak, practically compensates the difference in the atomic fluxes, as it is expected from the LeChatelier-Braun principle: the diffusion induced stresses compensate the effect generating them. This results in a slowing down of the intermixing and to the slowing down of its first stage (sharpening).

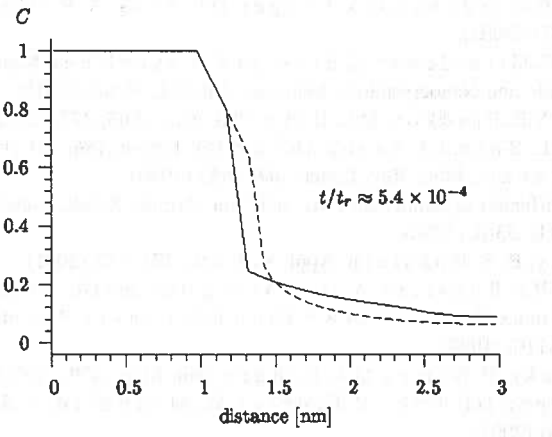

Fig. 10. Demonstration of the influence of the strength of the diffusional stress: $D_V/D_{Mo} = 2$ solid line, $D_V/D_{Mo} = 10$ dashed line

Acknowledgment

This work has been supported by the following Hungarian grants: OTKA T-038125, F-043372 and T-043464. C. Cserháti is a grantee of the "Bolyai János" scholarship.

REFERENCES

[1] I. Kaur, Y. Mishin, W. Gust, Fundamentals of Grain and Interphase Boundary Diffusion, London, J. Wiley & Sons, 1995.
[2] D.L. Beke, General Introduction, Diffusion in Semiconductors and Non-Metallic Solids Landolt-Bornstein, New Series, Berlin; ed. Beke D.L. 33-A, (1998).
[3] J. Bernardini, D.L. Beke, Diffusion in Nanomaterials in Nanocrystalline Metals and Oxides: Selected Properties and Applications; Eds. P. Knauth and J. Schoonman; Kluwer Publ. Boston (2001).
[4] S. Divinski, J.-S. Lee, Chr. Herzig, Nanodiffusion, special issue of Journal of Metastable and Nanocrystalline Materials; Ed. D.L. Beke, (2004).
[5] B. S. Bokstein, Nanodiffusion, special issue of Journal of Metastable and Nanocrystalline Materials; Ed. D.L. Beke, (2004).
[6] D.L. Beke, C. Cserhti, Z. Erdélyi, I.A. Szabó, Segregation in Nanostructures in Advances in Nanophase Materials and Nanotechnology Vol. Nanoclusters and Nanocrystals; Ed. H.S. Nalwa; American Scientific Publ. Califronia USA, (2003) p.211.
[7] J. Philibert, Atom Movements. Diffusion and Mass Transport in Solids, Les Ulms, France, Les Editions des Physique, Paris, (1991).
[8] I.V. Belova, G. E. Murch, Nanodiffusion, special issue of Journal of Metastable and Nanocrystalline Materials; Ed. D.L. Beke, (2004).
[9] D.L. Beke, G.A. Langer, A. Csik, Z. Erdélyi, M. Kis - Varga, I.A. Szabó, Z. Papp, Defect and Diffusion Forum, **194-199**, 1403 (2001).
[10] M. Bobeth, A. Ullrich, W. Pompe, Nanodiffusion, special issue of Journal of Metastable and Nanocrystalline Materials; Ed. D.L. Beke, (2004).
[11] D.L. Beke, Gödény, I., Erdélyi, G. Kedves, F.J. Phil. Mag. **A56**, 659 (1987).
[12] G. Erdélyi, W. Lokowski, D.L. Beke, Phil.Mag. **A56**, 672 (1987).
[13] S.V. Divinski, F. Hisker, Y.-S. Rang, J.-S. Lee, Chr. Herzig, Acta Mater. (2003) in press.
[14] J. C. M., Hwang, J. D. Pan, R. W. Balluffi, J. Appl. Phys., **50**, 1339 (1979).
[15] Z. Erdélyi, Ch. Girardeaux, G.A. Langer, D.L. Beke, A. Rolland, J. Bernardini, J. Appl. Phys. **89**, 3971 (2001).
[16] J. Bernardini C. Girardeaux, Z. Erdélyi, C. Lexcellent, Nanodiffusion, special issue of Journal of Metastable and Nanocrystalline Materials; Ed. D.L. Beke, (2004).
[17] B.S. Bokstein, V.E. Fradkov, D.L. Beke, Phil. Mag. **A65**, 277, (1992).
[18] C. Cserhati, D.L. Beke, I.A. Szabo, Def. and Dif. Forum, **156**, 121,(1998).
[19] P. Desre, A.P. Yavari, Phys. Rev. Letters, **64**, 1553 (1990).
[20] N. Stolwijk, Diffusion in Semiconductors and Non-Metallic Solids, Landolt-Bornstein, New Scries, Berlin; ed. Beke D.L. **33-A** (1998).
[21] A. S. Ostrovsky, B. S. Bokstein, Appl. Surf. Sci., **173**, 312 (2001).
[22] N. Balandina, B.S. Bokstein, A. Ostrovsky, Def. and Dif. Forum, **143-147**, 1499 (1997).
[23] D.L. Beke, P. Nemes, Z. Erdélyi, I.A. Szabó, D.G. Langer, Proc. of MRS Spring Meeting, San Francisco, **527**, 99-110, (1998).
[24] Z. Erdélyi, D.L. Beke, P. Nemes, G.A. Langer, Phil. Mag. **A79**, 1757 (1999).
[25] A. Csik, G. Langer, D.L. Beke, Z. Erdélyi, M., Menyhárd, A. Sulyok, Journal of Appl. Phys. **89**/1, 804-806 (2001).
[26] Z. Erdélyi, C. Girardeaux, Zs. Tökei, D.L. Beke, C. Cserháti, A., Rolland, Surf. Sci **496**, 129 (2002).

[27] Z. Erdélyi, D.L. Beke, I.A. Szabó, Phys, Rev. Letters **89**, 165901 (2002).
[28] Z. Erdélyi, D.L. Beke, Phys. Rev. **B.68**, 092102 (2003).
[29] Z. Erdélyi, G. Katona, D.L. Beke, submitted to Phys. Rev. B.
[30] D.L. Beke, Z. Erdélyi, I.A. Szabó, C. Cserháti, Nanodiffusion, special issue of Journal of Metastable and Nanocrystalline Materials; Ed. D.L. Beke, (2004).
[31] G. Martin, Diffusion in Materials (eds. A.L. Laskar J. C. Bocquet, G. Brebec, C. Monty) Nato ASI Series Series E Applied Sciences, ,Kluwer Academic Press, Dordrecht **179** 129 (1990).
[32] A.L. Greer, F. Speapen, *Synthetic Modulated Structures* (Eds. Chang, L.L. and Giessen, B.C.), Academic Press, New York, p. 419 (1985).
[33] A. Saúl, B. Legrand, G. Tréglia, Surf. Sci. **331-333**, 805 (1995).
[34] S. Delage, B. Legrand, F. Soisson, A. Saúl, Phys. Rev **B58**, 15810 (1998).
[35] J. M. Roussel, A. Saúl, G. Tréglia, B. Legrand, Phys. Rev. **B60**, 13890 (1999).
[36] D.E. Jesson, *Handbook of Thin Film Process Technology,* Eds. D.A. Glocker, S.I. Shah; IOP Publishing Ltd. Bristol and Philadelphia, (1997) p. F1:1.
[37] G.B. Stephenson, Acta Metall. **36**, 2663 (1988).

Received: 1 March 2004.